Displacement Measurement System and Control of Ionic Polymer Metal Composite Actuator

KYRIAKOS TSIAKMAKIS, VASILEIOS DELIMARAS, ARGYRIOS T. HATZOPOULOS,
MARIA S. PAPADOPOULOU
Department of Information and Electronic Engineering
International Hellenic University
Thessaloniki
GREECE

Abstract: - This work presents a study comparing two control methods used in IPMC actuators. The position of the free end of the actuator is extracted using low-frequency signals, and the driving voltage is limited to ±3 V. This paper also proposes a new image sensor-based method for measuring displacement, which uses the actuator's route and applied current to predict the direction and detect the free edge using small areas of interest. The algorithm detects the area of the moving route, reduces the searching area of the IPMC's free edge, and predicts the edge direction. An experimental setup was established using a laser sensor and camera system. The results of simple computer usage reveal that the new technique is 17% faster. The paper also discusses model identification using a black-box approach. A major objective is to find the optimal control settings for various methods to highlight the issue of saturation and define the duration in which the IPMC actuator can be controlled.

Key-Words: - displacement measurement, image sensor, laser sensor, control of robotic actuator, PID, MRAC

Received: November 13, 2022. Revised: April 19, 2023. Accepted: May 13, 2023. Published: June 12, 2023.

1 Introduction

Ionic Polymer-Metal Composite (IPMC) is a type of smart material that exhibits bending deformation when an electric potential is applied, [1]. These strips have found applications in various fields, including biomechanics, automobiles, and robotics, [2].

An application of IPMCs as actuators in the environment is the development of artificial muscles for soft robotics. IPMCs can be used as actuators in soft robots, enabling them to move and manipulate objects in the environment, [3].

The IPMC actuators have been employed in the development of water and airflow control systems in the environment and can be used as pumps and valves, controlling the flow of fluids and gases. Can be used in water treatment plants to control the flow of water and ensure that it is properly treated before being released back into the environment, [4].

The development of devices that can simulate the movements of living organisms, such as fish or birds, is one area of interest for environmental monitoring and exploration. It is possible to create robotic machines that can fly or swim in the air or water using IPMC actuators, [5], [6].

One important aspect of using IPMC strips is the need for accurate position measurement and control, [7]. Research in position measurement and control of IPMC strips has focused on developing techniques and control algorithms to accurately track and control the position of the strip. Control methods have also been developed that use feedback from these sensors to control the position of the strip. These methods typically use a proportional-integral-derivative (PID) controller or an adaptive controller to adjust the applied electric potential and maintain the desired position of the strip, [8], [9]. These techniques use mathematical models of the IPMC strip to predict its behavior and adjust the applied electric potential in real-time to achieve the desired position. Overall, research in position measurement and control of IPMC strips is an important area of study that has the potential to advance the use of these smart materials in various fields, [10]. IPMC strip position measurement and control research is a rapidly evolving field with numerous applications in a wide

range of industries. In the future, the field of IPMC strips will continue to advance through the development of new fabrication techniques, control approaches, and exploration of new applications, [11].

In this work, two control methods are compared and presented. Step or low-frequency square signals are specifically applied to the control systems. Many researchers extract the position of the free end of the strip without considering the high increment of the applied voltage. The driving voltage of the IPMC actuator is limited to |3 V| due to higher voltage the plant will be destroyed. In this paper, the simulation results with and without this saturation are presented. The study and development of these methods showed that it is possible to accurately control the position until the applied voltage does not exceed the amplitude of ±3 V.

There are several methods for displacement measurement of Ionic Polymer-Metal Composites (IPMCs), including using a laser, a camera, or an integrated sensor. This laser method can provide high accuracy and resolution, but it requires expensive equipment and is sensitive to environmental factors such as temperature and vibration and bigger displacements, [12].

The camera system involves using a low-cost camera to capture images of the IPMC and analyze the displacement based on the image data. This method is non-contact and can provide high spatial resolution, but it requires careful calibration and is sensitive to lighting conditions and camera settings, [13].

The integrated sensor method involves attaching a sensor to the IPMC and measuring the displacement based on the output of the sensor. This method can provide high accuracy and is relatively simple and inexpensive, but it requires direct contact with the IPMC and may not provide high spatial resolution, [14].

A new image sensor-based method for measuring displacement is presented. The new algorithm uses the route of the actuator and the applied current to predict the direction and detect the free edge using small areas of interest. The algorithm reduces the search area by creating small overlapping regions. Edge detection techniques are applied to these small areas to locate the free edge of the IPMC.
The algorithm performs gray-scale and clipping, followed by edge detection and feature edge detection. It distinguishes the IPMC strip from the background, determines the edge, and identifies the region surrounding the edge.

In this work, the problem of saturation in the applied driving voltage of the IPMC is presented. The control can hold its position steady for a short time until the voltage reaches the value |3 V|. One of the main objectives of the work is to identify the settings needed by each control method to be able to control the position of an IPMC with different geometric characteristics for a longer period of time. Depending on the time it can be kept in a stable position, IPMC actuators can be employed in robotic systems for precise positioning and manipulation tasks. By implementing position control, IPMC actuators can be used to control the movement of robotic limbs, grippers, or other end-effectors. This application is particularly useful in scenarios where delicate and precise movements are required, such as in medical robotics or assembly operations.

2 Measurement Method

An experimental setup was established using a laser sensor and a camera system, as shown in Fig.1. The setup was driven with low-frequency voltage signals (up to 100 mHz) using a computing system and a current amplifier that generated sinusoidal, square, and step signals. The captured image of the movement was then digitized through an image processing algorithm, which plays a crucial role in the proposed visual measurement technique. One IPMC sample was tested in water.

The experimental setup involves the use of a camera with a frame rate of 60 frames-per-second and a resolution of 640×480 pixels per frame. The camera was employed to monitor the movement of the IPMC (Nafion/Li+) actuator strip of length 2.5 cm.

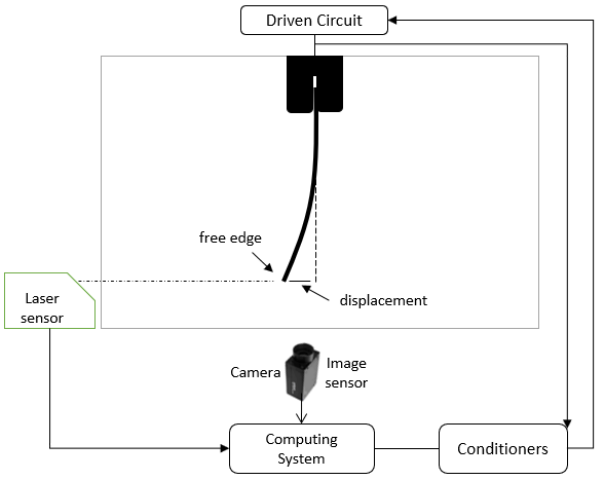

Fig. 1: Experimental setup for measuring the displacement of IPMC actuators

Accuracy is directly related to the resolution of the image. Experimental results show 1 pixel deviation between the marked and real point of interest. The image resolution of 640×480 pixels indicates a position error of about ±0.09 mm for this experimental setup.

A new method for measuring displacement is presented. The main procedure of the algorithm is the frame extraction and the calculation of the displacement from data. The procedure is fully automated for the detection of the free end edge of the IPMC actuator in each frame and provides a graphical display of the points required for the time-related computations.

The system exports the relevant frames with the corresponding time-stamps.

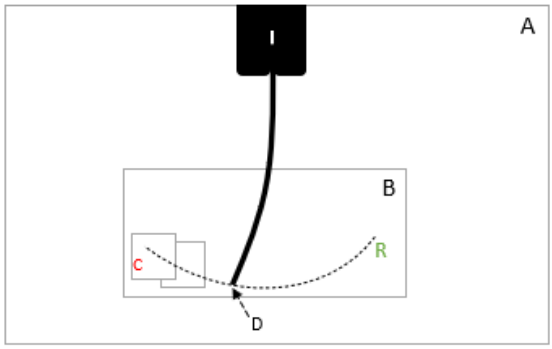

Fig. 2: The minimized area of interest and small regions

One way of determining the correlation between pixels and the actual size is to utilize a component in the viewing field as a point of reference, taking into consideration the camera's resolution and distance from the actuator.

The camera is placed perpendicular to the movement of the material and the region of interest is determined (B), as shown in Fig.2. At the beginning, the actuator is activated by applying a low-frequency sinusoidal signal and the algorithm detects the area of moving route (R). The purpose of this implementation is to reduce the searching area of the lower free edge of the IPMC.

Small overlapping areas (C) are created throughout the route. The goal is to apply edge detection techniques only to small areas. Then the algorithm reads the current provided by the external circuit and predicts the direction of the free edge. It can detect if the material is moving to the left or to the right and in the case of the step response (or control), it is necessary to detect when it holds at a steady state value.

Using the time and the value of the current value the algorithm chooses the appropriate small regions to locate the free edge. The edge detection algorithm has been described in the paper, [15].

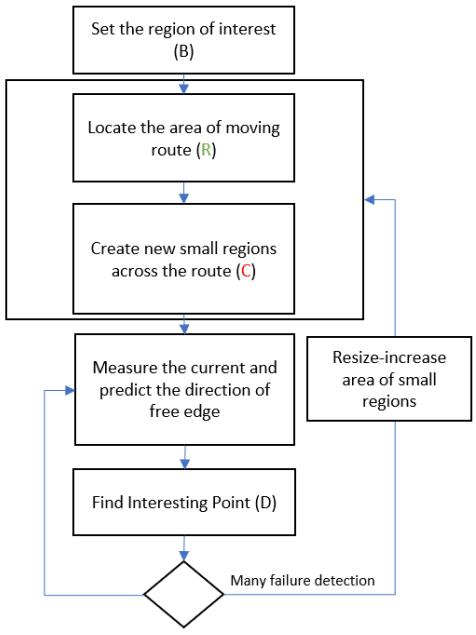

Fig. 3: Proposed block diagram of the process

If the algorithm fails many times to locate the edge, then an initial process to resize-increase the area of small regions or redetect the route is performed again, as shown in Fig.3.

The software then performs grayscale and clipping, followed by edge detection and feature edge

detection as the first steps in the extraction process for each small region. The grey-scale method was utilized to monitor the end of the strip under varying light conditions in comparison to the black-white. The location of the IPMC strip is then distinguished from the background by utilizing an automated process that employs an appropriate clipping method to concentrate on the area where the material is moving. The edge is then distinctly determined through surface tracing and edge detection, which also detects the spots required for calculating the displacement measurement.

The region surrounding the edge is identified using an image analysis algorithm. The procedure then determines the centre point from this region to correct for any inaccuracies caused by the actuator's thickness. The accuracy of these calculations is determined by the magnitude of the displacement. The procedure is calibrated, and the computer system automates the process, ensuring a precise relationship between the pixel difference and real-world difference. To ensure accurate image capture, the calibration procedure involves determining and adjusting the camera's internal properties and characteristics. This includes factors such as lens distortion, focal length, sensor size, and other characteristics that affect how the camera captures and interprets light. A calibration target or pattern with a defined size and features is used to calibrate a camera. Checkerboard patterns and specific calibration charts are common calibration targets. These targets serve as reference points throughout the calibration procedure. The camera's resolution is equal to 0.09mm when a specified field of view and distance between the camera and the actuator in mm are used. The software determines the number of pixels associated with the actuator and, with the knowledge of its exact size, calculates the correct relationship between pixels and actual length units.
The results of the new method showed that the new technique is 17% faster when using simple computer usage according to the research, [16].

3 Model Identification

The inherent difficulties of performing experiments under underwater conditions, combined with the difficulty in determining the transduction effect of an IPMC actuator, make obtaining a physical or grey box model extremely challenging. As a result, this research takes a black-box approach. The goal of this method is to estimate the coefficient values of a priori well-determined transfer function. The coefficients are calculated empirically by comparing experimental data to transfer function evaluations.

The IPMC-based cantilever's step response must be measured first. Fig.4 shows the results of the experiment. Using the sweep plus step response signal, the model is estimated and identified throughout the identification process.

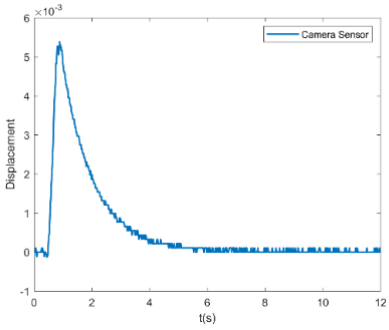

Fig. 4: Step response of IPMC measured by camera-based system

The estimation process compares the output of the model to a predetermined set of inputs and parameters. Using a cost function, the model's output is compared to the experimental data.

The cost function F_{cost} used is based on the mean squared error (MSE):

$$F_{cost} = \frac{1}{N}\sum_{i=1}^{N}(y_i - \hat{y}_i)^2 \qquad (1)$$

where y_i is the measured value, the $\hat{y}_i$ is the corresponding simulated value and the n is the number of samples. The parameters that minimize the cost function are determined using a cost function minimization algorithm. It's critical, to begin with the appropriate initial settings when using this type of identification procedure to ensure that the maximum frequency range is covered. Furthermore, certain numbers of periods are used in this evaluation for each of these signals to restrict the influence of noise sources.

To produce reliable identification results, the input signal must have sufficient power information in the frequency region where the model is identified. The outcome of the identification procedure is a fourth-order transfer function.

The identified fourth-order model is then reduced to a second-order model in the following function:

$$H(z) = \frac{5.25005\times10^{-5}z - 5.250045\times10^{-5}}{z^2 - 1.99125z + 0.99125} \quad (2)$$

The reduction of a fourth-order model to a second-order model is accomplished by the use of a specific technique and a related algorithm. Primary phases in the method include the comparison of poles with zeros, approximations of equal values, and adjustment of residual terms, all of which are necessary. Although a fourth-order model accurately represents the behavior of IPMC, we must avoid intricate computations that result in time-consuming calculations. A simplified approach to system analysis is achieved by the use of a reduced second-order model, which provides almost the same accuracy in the description of the system's behavior as the original model. The frequency range of interest is below 1 Hz, which is where the great majority of underwater robotic applications operate.

After obtaining the IPMC actuator's open loop model, a reference model may be presented to characterize the system's expected dynamic behavior in closed loop operation.

The purpose of model reduction is to operate independently of frequency resonance and to simplify mathematical computations.

Experiments and simulations have revealed that the majority of model constraints in the second order, particularly at low frequencies, are decreased. While a simplified model without resonance frequency is simple to create and use in real-time control systems, it does not accurately represent the model's behavior and may result in unstable situations, particularly for long IPMC samples. As a consequence, the strategy that results in a lower order model and eliminates the resonance frequency component is best appropriate for small length samples, and low frequencies where the influence of resonance is minor.

4 Results

4.1 Simulation Results

According to the specific transfer function of (2), two position control methods of the IPMC for step response are presented. The first uses a simple PID and the second a MRAC control presented in a previous study, [17].

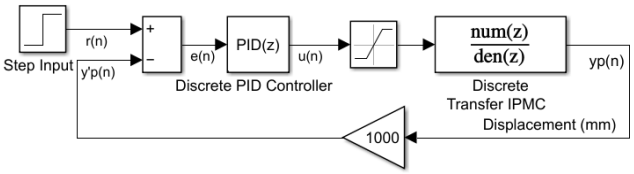

Fig. 5: PID control for IPMC actuator

The desired final value is achieved when simulated position control is applied, but a high plant input voltage is not considered. In this study, the input voltage, the equation of the discrete transfer function and the control diagrams are presented. The simple Discrete PID control is shown in Fig.5. At the system input, a step function is applied with a voltage amplitude that determines the controller's setpoint, denoted as $r(n)$, aiming to achieve the desired displacement at the plant's output $y_p(n)$. The error, denoted as $e(n)$, is then calculated as the difference between the setpoint and the actual displacement, that is, $e(n) = r(n) - y_p'(n)$. It is important to note that the output $y_p(n)$ is multiplied by a suitable factor $\alpha = 1000$ to scale it to the same order of magnitude as the amplitude of the input voltage $r(n)$. Subsequently, using the error $e(n)$, the discrete PID outputs a signal that controls the plant's input, denoted as $u(n)$, which is limited to a maximum of ± 3 V before being applied to the IPMC. The optimization algorithm Taguchi is used to determine the parameter values K_p, K_i, and K_d, [18].

Fig. 6 and Fig.7 show the simulated response of the PID control system to a step input signal without applied voltage saturation for a duration time of 100 s and 1 s respectively. In the middle part of the figure, the error computed as the difference between input voltage and displacement is shown. The output value remains at a constant value but the applied voltage of the plant increases to high values. Similar results for a simulated 100 mHz square signal without applied voltage saturation are shown in Fig.8.

Fig. 9 shows the simulated response of the PID control system to a step input signal with applied voltage saturation for a duration time of 20 s. The output value remains at a constant value up to 12.3 s. This saturation prevents the application of low-frequency signals. The simulated response of PID control for 100 mHz input square signal with applied voltage saturation is shown in Fig.10. The frequency of the input signal is above the lower limit, the output value remains at a constant value and the applied

voltage of the plant increases to saturation value without causing instability.

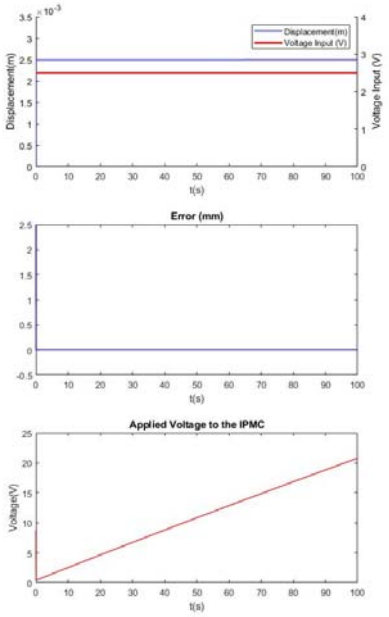

Fig. 6: PID - Simulation for 100 s - Step response without applied voltage saturation: displacement, error and applied voltage

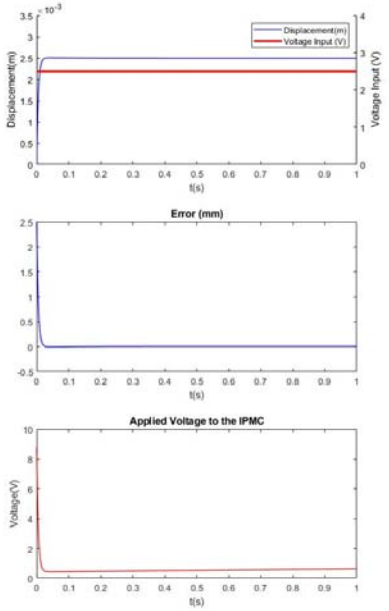

Fig. 7: PID - Simulation for 1 s - Step response without applied voltage saturation: displacement, error and applied voltage

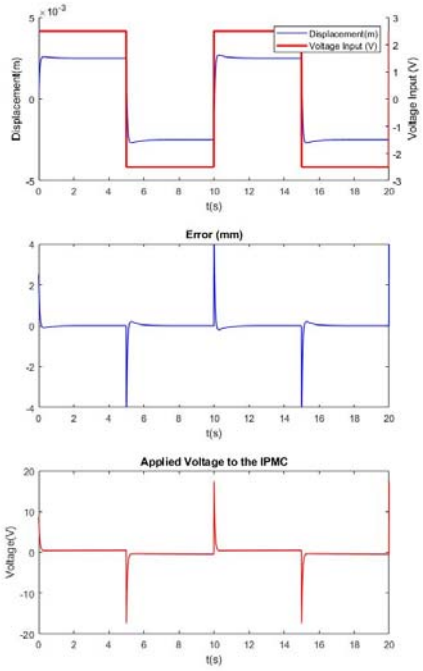

Fig. 8: PID - Simulated 100 mHz square signal without applied voltage saturation: displacement, error and applied voltage

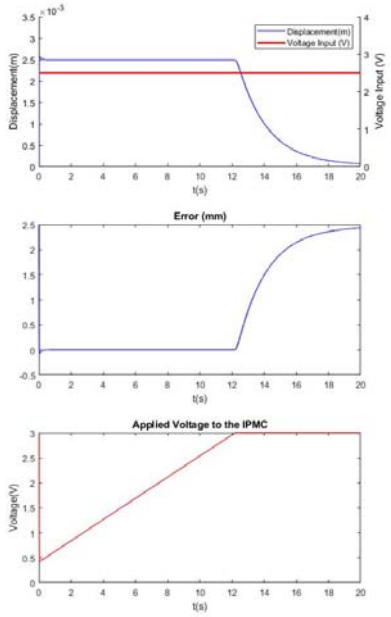

Fig. 9: PID - Simulation for 20 s - Step response with applied voltage saturation: displacement, error and applied voltage

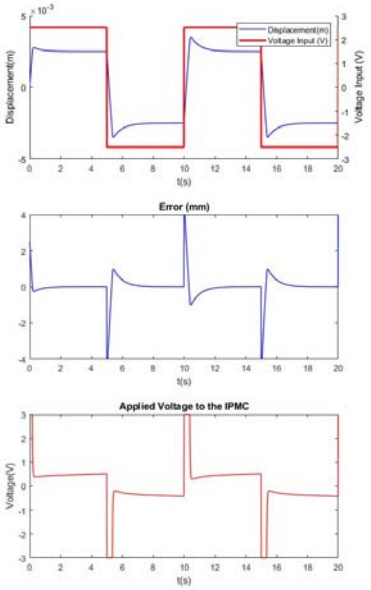

Fig. 10: PID - Simulated 100 mHz square signal with applied voltage saturation: displacement, error and applied voltage

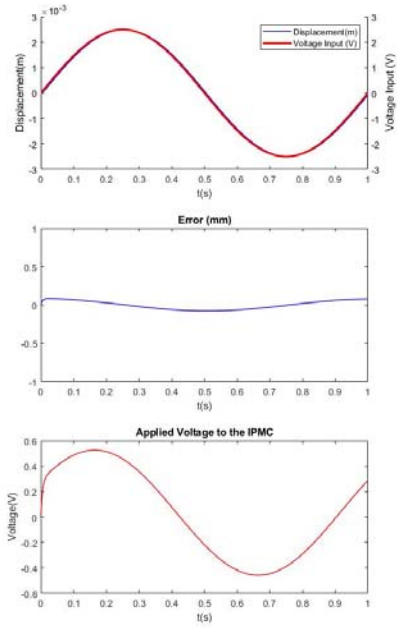

Fig. 11: PID - Simulated 1 Hz sinusoidal signal with applied voltage saturation: displacement, error and applied voltage

The simulated response of PID control for 1 Hz sinusoidal signal with applied voltage saturation is presented in Fig.11. The saturation problem does not appear for sinusoidal signals because the voltage at the input of the plant adapts faster to low values.

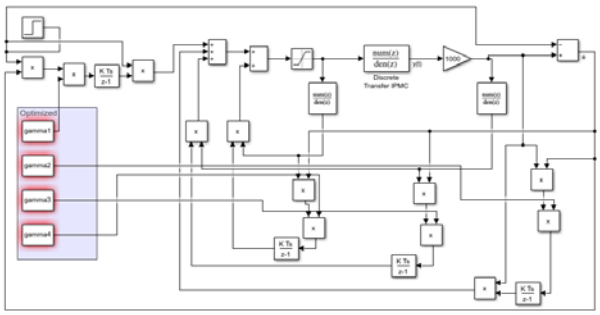

Fig. 12: MRAC control for IPMC actuator

The block diagram system of MRAC control for IPMC actuator is presented in Fig.12. The four gamma constants (γ_1, γ_2, γ_3, and γ_4) are set by an optimization algorithm, as reported in a previous study, [17].

Fig. 13 shows the simulated response of the MRAC system to a step input signal without applied voltage saturation for a duration time 100 s. The output value remains at a constant value, but the applied voltage of the plant increases to high values up to 20 V.

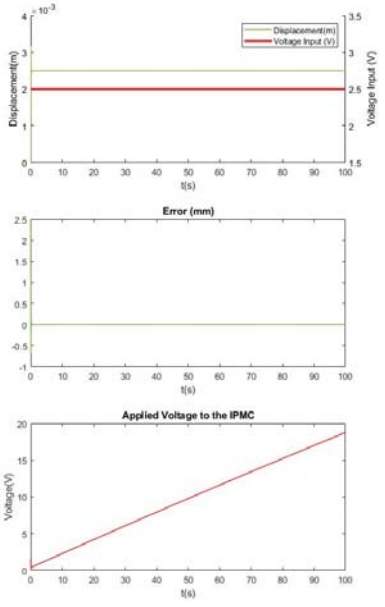

Fig. 13: MRAC - Simulation for 100 s - Step response without applied voltage saturation: displacement, error, and applied voltage

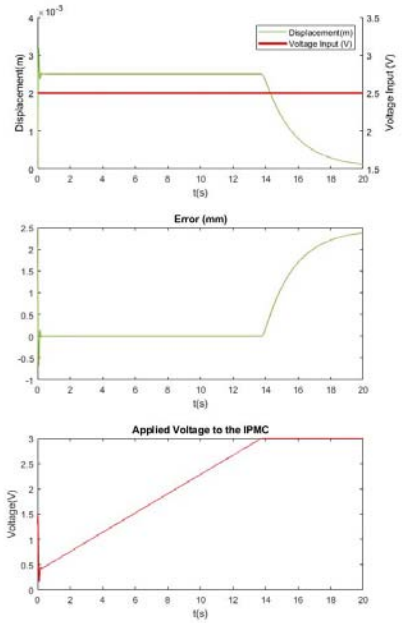

Fig. 14: MRAC - Simulation for 20 s - Step response with applied voltage saturation: displacement, error and applied voltage

Fig. 14 shows the simulated response of the MRAC system to a step input signal with applied voltage saturation for a duration time of 20 s. The output value remains at a constant value up to 13.8 s. It appears that MRAC shows a slight improvement over PID.

4.2 Experimental Results

In this chapter, the experimental results of the two controls with the use of voltage saturation for a simple step response are presented.

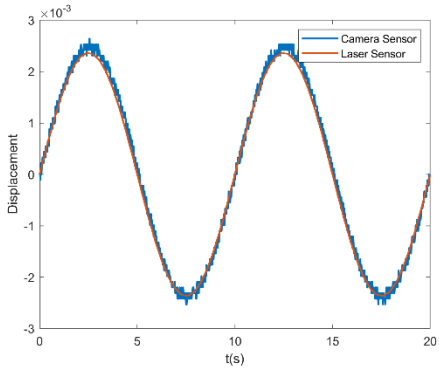

Fig. 15: Measuring displacement camera and laser-based system

In Fig.15 the displacement measured with both systems, camera and laser-based, when a sinusoidal input voltage is applied with an amplitude of 0.5 V is presented. At the operating frequency, the camera sensor-based measurement system is comparable to the laser sensor-based measurement system. There is no significant phase slip observed, nor a significant difference in the measurement of displacement between the two methods. However, at the peaks of the sine wave, an underestimation of the displacement measurement by the laser sensor is expected. As the point of interest (i.e., the free end of the IPMC) moves away, the laser sensor measures slightly closer to the fixed end of the IPMC, which exhibits less bending.

Fig. 16 shows the experimental step response graph produced by the camera-based system when PID control is applied with voltage saturation. The output value remains at a constant value up to 12.2 s. Once this time has elapsed, the output of the PID reaches a maximum value of 3 V and is unable to effectively maintain the displacement of the IPMC.

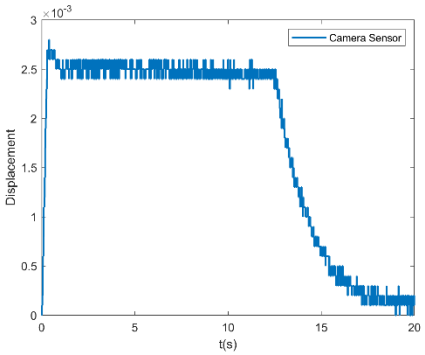

Fig. 16: PID control - Experimental step response with a camera-based system

The Taguchi-method optimized parameter values K_p, K_i, and K_d are different from the values set in the simulation.

This is due to the time required for processing between the two frames and the input voltage applied to the actuator through feedback to the PID controller is dependent on the frame rate.

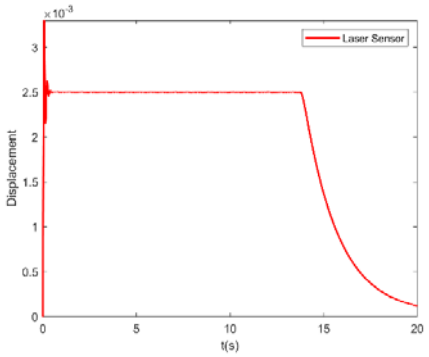

Fig. 17: MRAC control - Experimental step response with a laser-based system

The graph with experimental step response, when MRAC control is applied with voltage saturation, is shown in Fig.17. The output value remains at a constant value up to 13.5 s. The optimized parameters gamma (γ_i) have been obtained using the same optimization method as in the case of the PID controller. The MRAC controller managed to maintain the displacement of the IPMC for an additional 1.3 seconds compared to the PID.

Fig. 18 shows the graph with an experimental 100 mHz square signal when PID control is used with voltage saturation and concludes that the camera satisfactorily monitors the movement of the actuator.

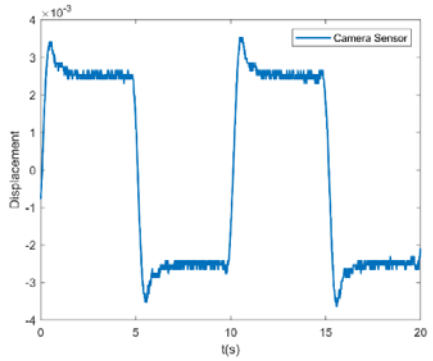

Fig. 18: PID - Experimental 100 mHz square signal with applied voltage saturation

5 Conclusion

The research described in the paper aims to find the optimal settings for different control methods to highlight this saturation problem and extend the period during which the IPMC actuator can be effectively controlled.

The ability to maintain the position of the IPMC actuator stable for an extended duration is critical for its use in robotic systems. The IPMC actuator can be used to precisely control the movement of robotic grippers by performing position control. To enable more efficient and reliable positioning and manipulation in robotic systems, the research's main objective is to identify the optimums control settings that enable IPMC actuators to operate reliably and under control for extended periods of time.

In order to accurately control the position of the free end of the strip until the applied voltage does not exceed the amplitude of ±3 V, the study proposed two control approaches for IPMC actuators using low-frequency signals.

A new image sensor-based method for measuring displacement was presented, which involved the use of an image processing algorithm and a camera system. For the experimental setup employed, the proposed technique was 17% faster and had an accuracy of ±0.09 mm.

The experimental setup, image processing technique, and control methods presented in this work contributed to the understanding and measurement of IPMC actuator displacement, to be used in robotic applications that require position control.

References:

[1] M. Shahinpoor and K. J. Kim, Ionic polymer-metal composites: I. fundamentals, Smart Materials and Structures, vol. 10, 2001, pp. 819-833.

[2] Bhandari, B., Lee, G.Y. and Ahn, S.H., 2012. A review on IPMC material as actuators and sensors: fabrications, characteristics and applications. International journal of precision engineering and manufacturing, 13, pp.141-163.

[3] Arena, P., Bonomo, C., Fortuna, L., Frasca, M. and Graziani, S., 2006. Design and control of an IPMC wormlike robot. IEEE Transactions on Systems, Man, and Cybernetics, Part B (Cybernetics), 36(5), pp.1044-1052.

[4] Nguyen, T.T., Goo, N.S., Nguyen, V.K., Yoo, Y. and Park, S., 2008. Design, fabrication, and experimental characterization of a flap valve IPMC micropump with a flexibly supported diaphragm. Sensors and Actuators A: Physical, 141(2), pp.640-648.

[5] Kamamichi, N., Yamakita, M., Asaka, K. and Luo, Z.W., 2006, May. A snake-like swimming

robot using IPMC actuator/sensor. In Proceedings 2006 IEEE International Conference on Robotics and Automation, 2006. ICRA 2006. (pp. 1812-1817). IEEE.

[6] Kim, H.I., Kim, D.K. and Han, J.H., 2007, April. Study of flapping actuator modules using IPMC. In Electroactive Polymer Actuators and Devices (EAPAD) 2007 (Vol. 6524, pp. 359-370). SPIE.

[7] Z. Chen, X. Tan, M. Shahinpoor, "Quasi-static Positioning of Ionic Polymer-Metal Composite (IPMC) Actuators," Proceedings of the IEEE/ASME International Conference on Advanced Intelligent Mechatronics, 2005.

[8] Fang, B.K., Ju, M.S. and Lin, C.C.K., 2007. A new approach to develop ionic polymer–metal composites (IPMC) actuator: Fabrication and control for active catheter systems. Sensors and Actuators A: Physical, 137(2), pp.321-329.

[9] Brufau-Penella, J., Tsiakmakis, K., Laopoulos, T. and Puig-Vidal, M., 2008. Model reference adaptive control for an ionic polymer metal composite in underwater applications. Smart Materials and Structures, 17(4), p.045020.

[10] Farid, M., Gang, Z., Khuong, T.L., Sun, Z.Z., Ur Rehman, N. and Rizwan, M., 2014. Biomimetic applications of ionic polymer metal composites (IPMC) actuators-a critical review. Journal of Biomimetics, Biomaterials and Biomedical Engineering, 20, pp.1-10.

[11] Aabloo, A., Belikov, J., Kaparin, V. and Kotta, Ü., 2020. Challenges and perspectives in control of ionic Polymer-Metal Composite (IPMC) Actuators: A Survey. IEEE Access, 8, pp.121059-121073.

[12] Palmre, V., Kim, S.J., Pugal, D. and Kim, K., 2014. Improving electromechanical output of IPMC by high surface area Pd-Pt electrodes and tailored ionomer membrane thickness. International Journal of Smart and Nano Materials, 5(2), pp.99-113.

[13] Sun, Q., Han, J., Li, H., Liu, S., Shen, S., Zhang, Y. and Sheng, J., 2020. A miniature robotic turtle with target tracking and wireless charging systems based on IPMCs. IEEE Access, 8, pp.187156-187164.

[14] Yamakita, M., Sera, A., Kamamichi, N., Asaka, K. and Luo, Z.W., 2006, May. Integrated design of IPMC actuator/sensor. In Proceedings 2006 IEEE International Conference on Robotics and Automation, 2006. ICRA 2006. (pp. 1834-1839). IEEE.

[15] Tsiakmakis, K. and Laopoulos, T., 2011. An improved tracking technique for visual measurements of ionic polymer–metal composites (IPMC) actuators using Compute Unified Device Architecture (CUDA). Measurement Science and Technology, 22(11), p.114006.

[16] Tsiakmakis, K. and Laopoulos, T., 2011, September. Comparison of improved methods for tracking movements of IPMC actuators. In Proceedings of the 6th IEEE International Conference on Intelligent Data Acquisition and Advanced Computing Systems (Vol. 1, pp. 467-472). IEEE.

[17] Tsiakmakis, K., Delimaras, V., Hatzopoulos, A.T. and Papadopoulou, M.S., 2023. Real Time Discrete Optimized Adaptive Control for Ionic Polymer Metal Composites. WSEAS Transactions on Systems and Control, 18, pp.26-37.

[18] Sonawane, P., Savakhande, V.B., Chewale, M.A. and Wanjari, R.A., 2018, January. Optimization of PID controller for Automatic voltage regulator system using Taguchi method. In 2018 International Conference on Computer Communication and Informatics (ICCCI) (pp. 1-6). IEEE.

Contribution of Individual Authors to the Creation of a Scientific Article (Ghostwriting Policy)

The authors equally contributed in the present research, at all stages from the formulation of the problem to the final findings and solution.

Sources of Funding for Research Presented in a Scientific Article or Scientific Article Itself.

No funding was received for conducting this study.

Conflict of Interest

The authors have no conflict of interest to declare.